CFD simulation of wettability of laser-structured surfaces

Jan Novosád[1,*], *Libor* Dvořák[1] and *Pavel* Peukert[1]

[1]VÚTS, a.s., Svárovská 619, 460 01, Liberec, Czech Republic

Abstract. This paper describes the numerical analysis of the wettability of the micro structured surfaces. The structure of the surface are the grooves created by the laser ablation. The main goal is to find the influence of the groove parameters on the wettability, specifically the contact angle. Ansys Fluent using the VOF method for multiphase simulation is used. In total, five different structures were investigated. The work started with the validation of the CFD methodology based on the experimental data for some structures. The CFD analysis was then performed. The fields of volume fraction as a results have been assessed to reach the contact angle value. The influence of structure parameters on the contact angle value were discussed. Finally, the recommendations for the optimal structure were defined.

1 Introduction

Creating functional surfaces with ultra-short pulse lasers is currently a very rapidly developing field of surface finishing. Lasers can achieve specific surface properties of various materials. It is a controlled process with high repeatability. Thus, a change in wettability, a reduction in the coefficient of friction or an improvement in biocompatibility can be achieved on the surface. Other properties that can be influenced by ultra-short pulse lasers include hardness, surface residual stress, or optical properties [1].

With sufficient intensity of the laser beam focused on the surface, material ablation occurs. Then the material evaporates and a controlled surface texture can be achieved. During the so-called "cold ablation", the material evaporates at the point of impact of the laser beam, but the surrounding material remains thermally unaffected. Hence this can be used to create very precise structures with picosecond or femtosecond lasers.

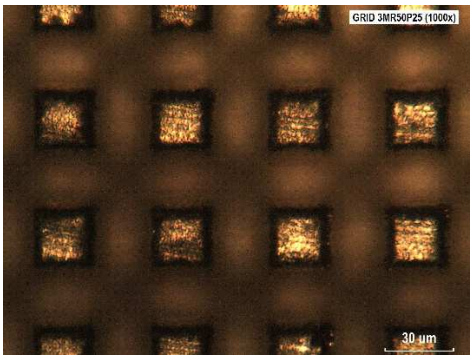

Fig. 1. Grid textured surface (grid) – fs laser, mag. 1000x.

For such surfaces, it is then necessary to analyse the achieved properties influenced by the action of the laser [1]. Also, surface texturing (see ex. on figure 1) with ultra-short laser pulses enables the creation of microstructures on a wide range of materials, including metal, ceramic and polymeric materials [2].

Titanium alloy (Ti grade V) was used for our experiment due to its mechanical properties and high biocompatibility. It is often used in biomedicine, e.g. as a joint replacement, dental implant or different types of microelectronics [3].

Implant infection and failure may occur during implementation. Infection is often caused by contamination of the surgical environment during implementation. The presence of bacterial colonies may prevent proper osseointegration. Consequently, it is important to reduce the likelihood of colonization of the implant surface through bacteria by providing these surfaces with antibacterial properties. Bacteria are sensitive to surface properties such as topography, chemical composition and wettability [2]. Our work focuses on the impact of the surface shape on wettability.

Wettability is the property of a liquid to adhere to the surface of some solids. Surface wetting is influenced by many circumstances such as surface roughness, surface finish, material, etc. Furthermore, wettability is affected by the surface tension of the liquid. Surface tension is the effect by which the surface of liquids strives to reach the lowest energy state [4]. Finally, a drop forms a spherical cap lying on the surface with a contact angle θ [4]. Then the surfaces are referred based on the contact angle value (see figure 2) to as hydrophilic ($\theta < 90°$),

* Corresponding author: jan.novosad@vuts.cz

hydrophobic ($\theta > 90°$) and super hydrophobic ($\theta > 150°$).

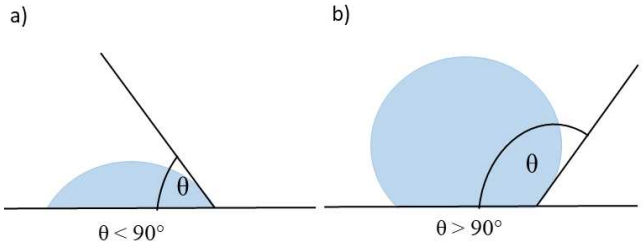

Fig. 2. Hydrophilic (a) and hydrophobic (b) surface.

The experimental investigation of the contact angle could be provided by several methods, including contact and optical systems [4], [5]. The shape of the flattened droplet is obviously measured and the contact angle is evaluated. Thus, the preparation of a sample with the surface texture is required.

Otherwise, the CFD (computational fluid dynamics) simulation could be used for investigation as the sample-free method. Wetting could be simulated as the multiphase problem when the liquid droplet falls in air onto the solid surface. The VOF (Volume of Fluid) method could be used to simulate thus type of multiphase problem [6]. The VOF method is often used successfully to model the behaviour of a drop on a solid surface. Nichita and Zun [7] have used the coupling of the VOF with dynamic contact angle. In recent years, numerical simulations have been used in research to investigate textured surfaces. The aim is to achieve hydrophobic or superhydrophobic surfaces [8], [9], [10].

2 Problem description

The main goal of our work was to prepare and validate the methodology of the numerical investigation of contact angle for the surfaces with microstructure textures. A schematic diagram of the phenomenon is shown in figure 3. Validation will be based on the experimentally investigated contact angle using the drop test. After that the validated methodology will be used to find the relationships between the parameters of the microstructure and the contact angle.

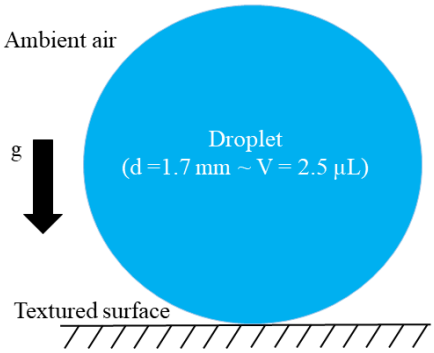

Fig. 3. Schematic diagram of falling droplet in contact with surface.

2.1 Geometry of the microstructure

This study is limited to the linear grooves structure only. The main parameters of the microstructure are shown in figure 4. Thus three parameters are defined, the pitch R, width of the groove P and height of the groove H.

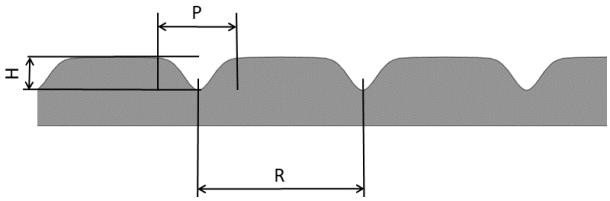

Fig. 4. Microstructure – sketch.

The shape of the groove corresponds to the Gaussian curve defined by:

$$f(x) = a\, e^{-\frac{(x-b)^2}{2c^2}} \quad (1)$$

where a = H, b = 0, c = P/6. In all solved cases the height H is 20 µm. Other parameters varies following the values in table 1. The grid of grooves was composed as two mutually perpendicular linear structures (see figure 1).

Table 1. Structures – main parameters and description.

Label	R (µm)	P (µm)	Groove type
1LR20P10	20	10	Linear
3MR50P25	50	25	Grid
1LR100P50	100	50	Linear
7LR100P20	100	20	Linear
xLR50P20	50	20	Linear

2.2 Model description

Some cases were investigated experimentally by the external laboratory in the past. The Surface Energy Evaluation System (See System [12]) was used. The volume of testing droplet was 2.5µL. As a result the contact angle value of structures 1LR20P10 ($\theta = 125.4° \pm 3.3°$) and 3MR50P25 ($\theta = 131.7° \pm 2.2°$) is known. These values can be used to validate the CFD simulation setup.

Following the situation on figure 3 the 3D domain were created respecting the parameters of the grooves. The boundaries were defined to be relevant to the reality and the spherical region was defined as the initial volume of the droplet (V = 2.5µL). Two symmetry planes were applied, therefore, the quarter model was used to speed up the computation. The dimensions of the quarter model were (2.5 x 2.5 x 2.5) mm.

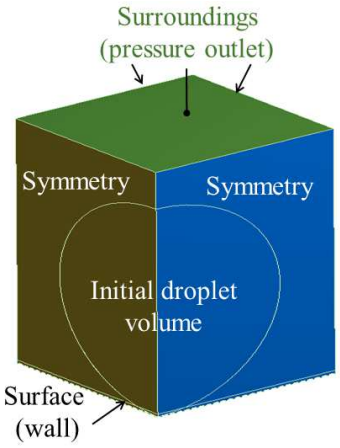

Fig. 4. Microstructure – sketch.

The tetrahedral grid was created using Ansys Meshing software. The grid refinement in the boundary layer region was used. Finally, the computational grid consists of around 2 mil. elements.

3 CFD simulation

For CFD simulations Ansys Fluent 2019 R2 were used. Multiphase flow was modelled by applying VOF model. The VOF model is a surface-tracking technique applied to a fixed Eulerian mesh. It is designed for two or more immiscible fluids where the position of the interface between the fluids is of interest. In the VOF model, a single set of momentum equations is shared by the fluids, and the volume fraction (VF) of each of the fluids in each computational cell is tracked throughout the domain [11]. In brief the volume fraction field is described by values between 0 and 1, where $VF_i = 0$ means no phase *i*, on the contrary $VF_i = 1$ means the volume is fulfilled by phase *i*.

For our case the two phase flow was modelled when the air as gas and water as liquid was used. Both with constant properties at 20°C. The laminar model is used. Gravity force ($g = 9.81$ m/s^2) was applied in the direction normal to the surface. The contact angle for flat surface (θ_0) have to been defined for the simulation. The values ranging from 72° to 84°, which are general tabular values for the titanium surface, have been applied to the textured surface.

The calculation is transient, the time-step was set to 10^{-7} s. The coupled scheme including the coupling with volume fractions was used for pressure velocity coupling. Body force weighted scheme was defined for pressure interpolation, second order scheme was used for momentum and compressive scheme for volume fraction was applied.

The criterion for convergence is defined as the area weighted average of volume fraction on the solid surface. The calculation stops, when the convergence criterion stabilizes over time. In other words the droplet falls onto the surface and forms a stable shape.

The CFD settings were unchanged for all analysed cases.

4 Results assesment

CFD simulation results are the fields of volume fraction. To be around the used count of elements the grid in outer region (far from the surface) is quite coarse, which causes relatively wide (diffuse) area of the interface between phases. For this reason the identify criterion for the interface was chosen to be $VF_{water} = 0.9$. It was supposed that the shape of the droplet could be described by two sections in planes of symmetry. In each plane the interface profile was exported as a set of points. First of all these points were fitted with a suitably selected curve that was defined by the equation:

$$f = ax^2 + bx + c, \tag{2}$$

with derivative,

$$f' = 2ax + b. \tag{3}$$

After that the derivative at the zero-point was calculated and used in the relation,

$$f'(0) = tg\ \theta, \tag{4}$$

from which the contact angle θ is evaluated. Finally the results from both symmetry planes are averaged to obtain the final value of contact angle.

The example of the set of interface points including the interpolation curve is shown in figure 5.

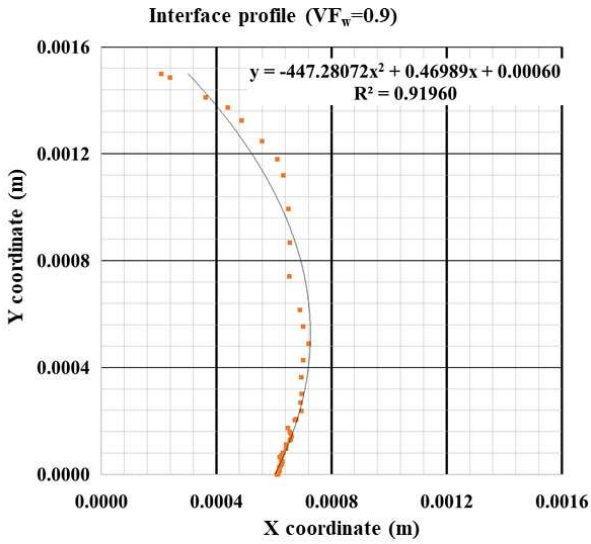

Fig. 5. Interface profile – example.

5 Results

The volume fraction $VF_{water} = 0.9$ was used to obtain the interface profile (points) from the CFD results. Based on these points the contact angle was assessed following the methodology described in chapter 4.

5.1 Validation results

3MR50P25 structure was investigated first. The values of θ_0 was set up to be {72°, 74° and 84°}. The angle θ_0 in the range between 72° to 74° gives the results close to the experimental data accordingly to the bar chart shown in figure 6. The deviation between the simulation and experimental data is lower than the measurement uncertainty, so the CFD setup could be considered as validated.

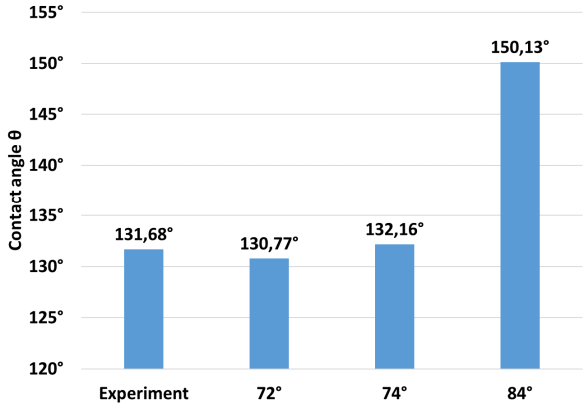

Fig. 6. Contact angle depending on θ_0 – structure 3MR50P25, θ_0 = {72°, 74° and 84°}.

To be sure with validation second calculation for 1LR20P10 structure was realized using the θ_0 = 74°. The results of validation is then shown in figure 7. To summarise, simulation results of both structures are in a good agreement with experimental data. The optimal value of the contact angle for flat surface which is set up is θ_0 = 74°.

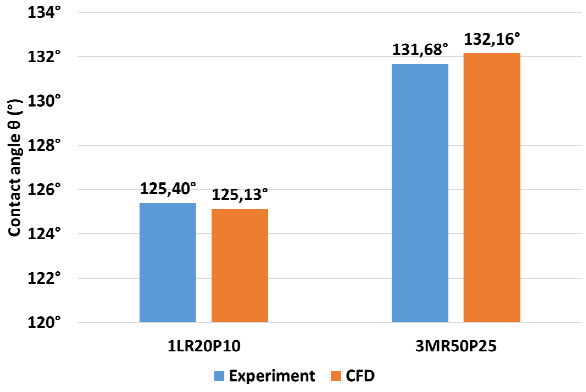

Fig. 7. Comparison between CFD results and experimental data – structures 1LR20P10, 3MR50P25, θ_0 = 74°.

5.2 Linear structures

The validated methodology (CFD setup) was used to investigate the influence of linear structure parameters onto the contact angle. Contact angle for flat surface was set up as θ_0 = 74°. Contact angle of the investigated structures 1LR100P50, 7LR100P20 and xLR50P20 was compared with the reference structure (1LR20P10). As a result the pitch and width of grooves significantly changes the value of contact angle (see figure 8).

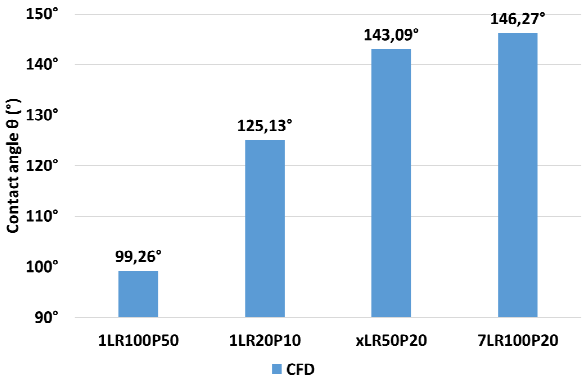

Fig. 8. Comparison of contact angle for different structures.

Unfortunately, there is not so much geometries to find the final statement about the influence of each parameter on the contact angle. However, it could show the trends and give us the ideas for choosing additional modification for testing. For this reason the influence of parameters on increase/decrease of the contact angle is our goal to design hydrophobic/hydrophilic structure.

Based on the available results (see figure 9), it can be concluded that increasing the width causes the significant decrease of contact angle. It is probably caused by decreasing the flat area in the space between grooves. Additionally, the fillet at the top of the groove where the groove merges into the straight part, is increasing. Thus, water can more easily flow into the groove, so the surface becomes less hydrophobic.

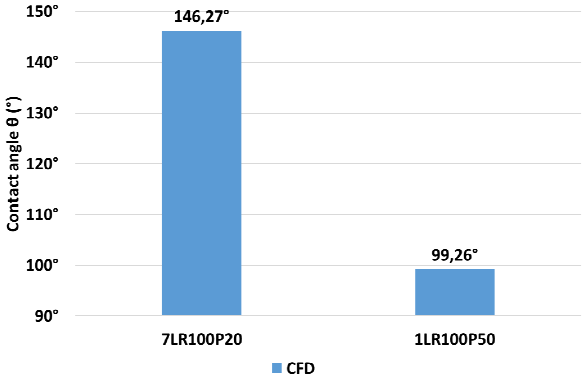

Fig. 9. Influence of the width of the grooves on contact angle (constant pitch R = 100 µm).

Otherwise the increase of the pitch (see figure 10) causes the increase of the contact angle. The contact area on the flat surface is larger with increasing the pitch.

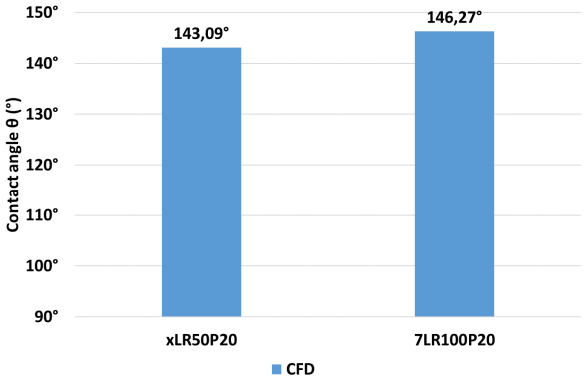

Fig. 10. Influence of the pitch between grooves on contact angle (constant width P = 20 µm).

Also the dimensionless R/P ratio could be set as a characteristic of the geometry. According to the comparison of all four cases (shown in figure 11) the increase of R/P leads to the increase of contact angle.

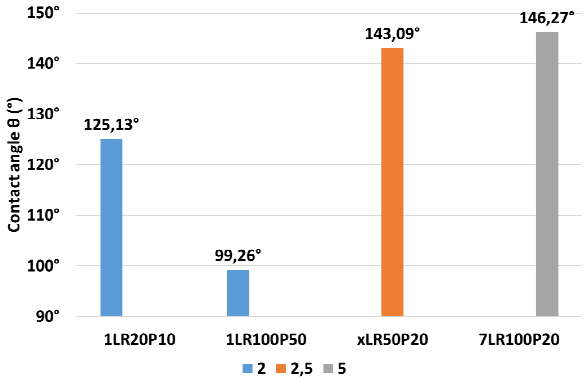

Fig. 11. Influence of the R/P parameter.

The studied cases results shows that the limit for maximum contact angle will be probably reached. Cn the contrary the infinite pitch creates the flat surface ($\theta \rightarrow \theta_0$).

6 Conclusion

For our work five different textured surface structures were selected for analysis. The main goal of the work was to analyse numerically the influence of individual structure parameters on the wettability, specifically the contact angle value. The experimental data exists for structures 1LR20P10 and 3MR50P25. Therefore the simulations of these structures had been solved firstly. CFD analysis based on the VOF method for multiphase have been created. The own simple methodology was used also for evaluating the contact angle from the field of volume fraction values. Validation of the CFD methodology was then performed by comparison with experimental data. Finally, three structures with different parameters of grooves geometry were simulated using the validated CFD setup.

The contact angle values were compared in different combinations to evaluate the effect of grooves width P, pitch R and the R/P ratio. However, the existence of results for only four variants of the line structure exist, the comparisons are always made for a very small number of variants. Therefore, it cannot be considered as meaningful for definitive conclusions.

Based on the available results, it can be concluded that increasing the width of the groove will significantly reduce the contact angle. This fact is probably related to a significantly changed geometry (larger fillet) at the top of the groove, where the groove merges into the straight part (flat surface). Thus, water can more easily flow into the groove, so the surface becomes less hydrophobic. Increasing the groove pitch, while the groove width is the same, shows a slight increase in contact angle. Also the increase of R/P ratio causes the increase of the contact angle. At the same ratio the results show a more dominant effect of the groove width. In the variants examined, the contact angle was decreased even if the pitch was increased. The influence of the groove width is probably more dominant than the pitch.

To summarise, the highest contact angle should be reached on the structure with a larger pitch R and a small slot width P should be suitable. The optimal maximum value have to be found as a limit, however very high values of pitch creates the flat surface, for which the contact angle is quite small equally to the angle for flat surface.

All the above-mentioned dependencies are analyzed on the basis of a very small number of solved structures. In order to confirm the validity of the above conclusions, it would be appropriate to continue the analysis of other structural variants. At the end the final structure sample will be prepared and investigated experimentally to confirm the results of CFD analysis.

This publication was written at the VÚTS, a.s. with the support of the project FV30265 - „Laserové technologie pro mikrostrukturování bionických a funkčních povrchů pokročilých materiálů“. Our acknowledgment belongs to all donors that helped us to reach the results of the work.

References

1. Y. Cai, W. Chang, X. Luo, A. M. L. Sousa, K. H. A. Lau, Y. Qin et. al. Precision Engineering **52**, pp. 266-275 (2018).
2. A. Cunha, A. M. Elie, L. Plawinski, A. P. Serro, A. M, Botelho do Rego, A. Almeida, M. C. Urdaci, M.-Ch. Durrieu, R. Vilar et. al. Applied Surface Science **360**, pp 485-493 (2016).
3. Z. Yu, G. Yang, W. Zhang, J. Hu et. al. J. of Materials Processing Technology **255,** pp. 129-136 (2018).
4. P.-G. de Gennes, F. Brochard-Wyart, D. Quéré. *Capillarity and wetting phenomena*. ISBN 0-387-00592-7 (2004).
5. DataPhysics. In: Sessile drop method - Optical determination of the contact angle [online] (2016) [cit. 2018-08-25]. Available at: www.dataphysics-instruments.com/knowledge/understanding-interfaces/sessile-drop-method/
6. J. H. Ferziger, M. Perić. *Computational methods for fluid dynamics*, 3rd Ed. ISBN 3-540-42074-6 (2002).
7. B. A. Nichita, I. Zun, J. R. Thome. A VOF method coupled with a dynamic contact angle model for simulation of two-phase flows with partial wetting. 7th International Conference on Multiphase Flow, ICMF 2010, Tampa, FL, USA (2010).
8. S. Chun, Z. Chengchun, G. Meihong, L. Xueli, L. Yan, R. Luquan. Int. J. of Heat and Fluid Flow **74**, pp. 89-109 (2018).
9. Ch. Liu, L. Zhu, W. Bu, Y. Liang. Micron **107**, pp. 94-100 (2018).
10. X. Wang, D.-L. Sun, X.-D. Wang, W.-M. Yan. Int. J. of Heat and Mass Transfer **135**, pp. 235-246 (2019).
11. *ANSYS Fluent Theory Guide*, Release 2019 R2, Ansys Inc. (2019).
12. See System.
Available at:www.advex-instruments.cz